BEST: International Journal of Management, Information Technology and Engineering (BEST: IJMITE)
ISSN (P): 2348-0513, ISSN (E): 2454-471X,
Vol. 4, Issue 4, Apr2016, 17-36

RADIATION AND CHEMICAL REACTION EFFECTS ON MHD NATURAL CONVECTION FLOW PAST A MOVING VERTICAL PLATE EMBEDDED IN A POROUS MEDIUM WITH HEAT SOURCE AND CONVECTIVE SURFACE BOUNDARY CONDITION

E. HEMALATHA & N. BHASKAR REDDY

Department of Mathematics, Sri Venkateswara University, Tirupati, A.P., India

ABSTRACT

This paper focuses attention to study the effects of heat and mass transfer characteristics on steady MHD free convective flow of a viscous incompressible electrically conducting and radiating fluid past a moving vertical plate embedded in a porous medium in the presence of the heat source and chemical reaction with convective surface boundary condition. The hot fluid is in contact on the left surface of the plate, while the stream of cold fluid flows along the right surface. Using the similarity transformations, the governing equations are transformed into nonlinear ordinary differential equations, and then solved by Runge-Kutta method along with shooting technique. The velocity, temperature and concentration as well as the numerical values of skin friction coefficient, Nusselt number, plate surface temperature and Sherwood number for various material parameters are discussed and represented through graphs and tables. The present results are compared with the available literature, and found to be in good agreement.

KEYWORDS: Heat And Mass Transfer, Free Convection, Internal Heat Generation, Heat Source, MHD, Porous Medium, Radiation, Chemical Reaction, Convective Boundary Condition, Shooting Method

1. INTRODUCTION

The study of heat and mass transfer plays vital role in flows past or through porous media. It finds applications in several engineering and geophysical fields. For example in nuclear reactors, oil recovery, underground energy transport, geothermal reservoirs and thermal insulation. Bejan and Khair [1] presented the heat and mass transfer effects on free convection boundary layer flow embedded in a porous medium. By using series expansion combined heat and mass transfer by natural convection from a sphere embedded in a porous medium was studied by Lai and Kulacki [2]. Raptis *et al*. [3] and Lai and Kulacki [4] analyzed the effects of free convection heat and mass transfer on boundary layer flow past a vertical plate with suction and blowing in saturated porous medium.

The study of free convection under the influence of magnetic field has attracted the interest of many researchers in view of its application in geophysics and astrophysics. Huges and Young [5] gave an excellent summary of applications. Shanker and Kishan [6] studied the effect of mass transfer on MHD boundary layer flow past an impulsively started infinite vertical plate. Bhaskara Reddy and Bathaiah [7, 8] studied MHD effects on natural convection laminar flow of an incompressible viscoelastic fluid. Later, he analyzed the effect of MHD on forced and free convection flow through two parallel porous walls. Elabashbeshy [9] studied the effects of heat and mass transfer on MHD boundary layer flow past a vertical plate in presence of variable temperature and concentration. Helmy [10] studied effect of MHD on boundary layer flow of unsteady free convection past a vertical porous plate.

Radiative heat transfer in which heat is transmitted from one point to another without intervening medium and had became a significant branch of the engineering sciences and is an essential aspect of various scenarios in hazards, solar power, environmental, chemical, aerospace and mechanical engineering. Hossain and Takhar [11] studied the effect of radiation in a laminar mixed convection flow over a vertical plate with uniform surface temperature. Suneetha *et al.* [12] analyzed the effect of radiation on MHD laminar boundary layer free convection flow past an impulsively started vertical plate with variable surface temperature and concentration. Chandrakala [13] examined the free convective boundary layer flow of a viscous incompressible fluid with uniform heat flux in the presence of thermal radiation. Anki Reddy *et al.* [14] investigated the thermal radiation effects on hydro-magnetic flow due to an exponentially stretching sheet. Raptis [15] analyzed the effects of thermal radiation on free convective flow over a vertical infinite porous plate embedded in a porous medium by using a regular perturbation technique. Ishak [16] analyzed the effect of MHD on boundary layer flow due to an exponentially stretching sheet in presence of radiation. An unsteady free convection oscillatory flow past a moving vertical plate in presence of radiation was presented by Mansour [17]. Sajid and Hayat [18] examined the effect of radiation on the mixed convection flow past an exponentially stretching sheet. This problem was solved analytically by employing homotopy analysis. The same problem was solved by Bidin and Nazar [19] using numerical technique. Recently, Poornima and Bhasker Reddy [20] analyzed the radiation effects on MHD free convection boundary layer flow of nanoflow over a nonlinear stretching sheet. Makinde [21] studied numerically the effects of heat and mass transfer on boundary layer flow past a moving vertical porous plate in presence of thermal radiation.

Analysis of transport processes and their interaction with chemical reaction has the greatest contributions to many areas of chemical science. In many chemical engineering processes a chemical reaction occurs between a foreign mass and the fluid. Das *et al*. [22] analyzed the mass transfer along an impulsively started infinite vertical plate with the effects of heat flux and chemical reaction. Many authors studied the effect of chemical reaction on different geometries. Effects of chemical reaction heat and mass transfer, on laminar flow along a semi infinite plate were analyzed by Anjalidevi and Kandaswamy [23]. MHD mixed convection Hiemenz flow through porous media was studied by Seddeek *et al*. [24] by taking chemical reaction, variable viscosity and radiation in to account. Patil and Kulkarni [25] dicussed free convective flow of a micro polar fluid through a porous medium with heat generation. Gangadhar and Bhaskar Reddy [26] investigated hydro magnetic flow past a moving vertical plate embedded in a porous medium in the presence of suction and chemical reaction.

The study of heat source or sink is important in problems of exothermic and endothermic chemical reactions. Olanrewaju *et al.* [28] studied the effect of heat generation on thermal boundary layer with a convective surface boundary condition. Similarity solution of MHD flow past a vertical plate with convective boundary condition was obtained by Makinde[29]. Later he analyzed the effect of heat generation on the same problem [30]. Ibrahim *et al*. [31] analyzed an unsteady MHD free convection flow past a vertical moving plate by considering radiation, heat source, chemical reaction and suction. Hall current effects on MHD flow along a stretching vertical plate with chemical reaction, internal eat generation or absorption was analyzed by Salem and Abd El-Aziz [32].

In this paper an attempt is made to study the radiation effects on MHD free convective boundary layer flow of a viscous incompressible fluid over a moving vertical plate embedded in a porous medium and the combined effects of heat source and chemical reaction with convective surface boundary condition. The governing equations of the flow field are partial differential equations and these equations are reduced to a set of ordinary differential equations by using similarity

transformations, the resultant equations are coupled and non-linear, and hence are solved numerically by using the fourth order Runge - Kutta method along with shooting technique. The effects of various governing parameters on the velocity, temperature, concentration are presented graphically and discussed quantitatively. The local skin-friction coefficient, Nusselt number, plate surface temperature and Sherwood are computed numerically for variations in major parameters and reported in tables.

2. MATHEMATICAL ANALYSIS

We consider a steady two dimensional hydro magnetic flow of a viscous incompressible radiating stream of cold fluid past a semi infinite vertical moving plate embedded in a porous medium, in the presence of heat generation and absorption. The x-axis is taken in the direction of the flow and y-axis perpendicular to it. A uniform magnetic field of strength B_0 is considered in the transverse direction. The plate temperature and concentration are taken to be T_f and C_w, and the ambient temperature and concentration of the fluid are denoted by T_∞ and C_∞. The cold fluid on the right side of the plate is heated by convection from hot fluid provides heat transfer h_f and heat is generated internally at volumetric rate Q_0. The fluid is assumed to be of small electrical conductivity so that the magnetic Reynolds number is much less than unity and hence induced magnetic field can be neglected.

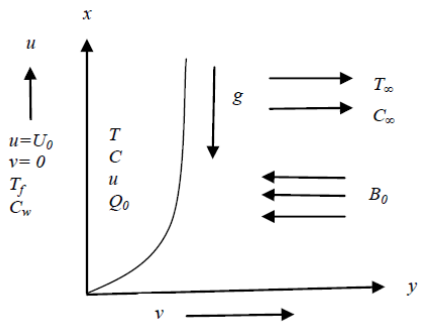

Figure 1: Schematic Diagram of the Physical Model

Under the above assumptions and usual Boussinesq's approximation, in the absence of input electric field, the continuity, momentum, energy, and concentration equations describing the flow can be written as

$$\frac{\partial u}{\partial x}+\frac{\partial v}{\partial y}=0 \tag{1}$$

$$u\frac{\partial u}{\partial x}+v\frac{\partial u}{\partial y}=\upsilon\frac{\partial^2 u}{\partial y^2}-\frac{\sigma B_0^2}{\rho}+g\beta\left(T-T_\infty\right)+g\beta^*\left(C-C_\infty\right)-\frac{\upsilon}{K}u \tag{2}$$

$$u\frac{\partial T}{\partial x}+v\frac{\partial T}{\partial y}=\alpha\frac{\partial^2 T}{\partial y^2}+\frac{Q_0}{\rho C_p}\left(T-T_\infty\right)-\frac{1}{\rho C_p}\frac{\partial q_r}{\partial y} \tag{3}$$

$$u\frac{\partial C}{\partial x}+\frac{\partial C}{\partial y}=D\frac{\partial^2 C}{\partial y^2}-Kr'C \tag{4}$$

where u and v denote the fluid velocity in the x - and y - directions respectively. T and C are the temperature and concentration of the fluid respectively, υ - the kinematic viscosity, σ - the electrical conductivity, ρ - the fluid density, g - the gravitational acceleration, β - the thermal expansion coefficient, β^* - the solutal expansion coefficient, K - the permeability of the porous medium, α - the thermal diffusivity, Q_0 - the heat source, C_p - the specific heat at constant pressure, q_r - the radiative heat flux, D - the mass diffusivity and Kr'- the rate of chemical reaction .

The boundary conditions for the velocity, temperature and concentration fields at the plate surface and far into the cold fluid are

$$\begin{aligned} &u(x,0) = U_0, \;\; v(x,0) = 0, \\ &-k\frac{\partial T}{\partial y}(x,0) = h_f\left[T_f - T(x,0)\right], \\ &C(x,0) = C_w = Ax^{\lambda} + C_{\infty}, \\ &u(x,\infty) = 0, \;\; T(x,\infty) = T_{\infty}, \;\; C(x,\infty) = C_{\infty}, \end{aligned} \tag{5}$$

Where C_w is the species concentration at the plate surface, A is the constant, λ is the power index of the concentration, U_0 is the plate velocity, k is the thermal conductivity of the fluid.

Following Brewster [33], applying Rosseland approximation, the heat flux q_r for the optically thick fluid can be written as

$$q_r = \frac{4\sigma^*}{3k^*}\frac{\partial T^4}{\partial y} \tag{6}$$

Here σ^* is the Stephen-Boltzmann constant and k^* is the mean absorption. Taking the temperature differences to be small, we linearize the equation (3) using Taylor expansion of T^4 about T_{∞}. After simplification we get

$$T^4 = 4T_{\infty}^3 T - 3T_{\infty}^4 \tag{7}$$

In view of the equations (6) and (7), the equation (3) reduces to

$$u\frac{\partial T}{\partial x} + v\frac{\partial T}{\partial y} = \alpha\frac{\partial^2 T}{\partial y^2} + \frac{Q_0}{\rho C_p}(T - T_{\infty}) + \frac{16\sigma^* T_{\infty}^3}{3k^*\rho c_p}\frac{\partial^2 T}{\partial y^2} \tag{8}$$

In order to write the governing equations and the boundary conditions in dimensionless form, the following dimensionless quantities are introduced.

$$\eta = y\sqrt{\frac{U_0}{\upsilon x}}, \;\; u = U_0 f'(\eta), \;\; v = -\frac{1}{2}\sqrt{\frac{\upsilon U_0}{x}}f(\eta) + \frac{U_0 y}{2x}f'(\eta),$$

$$\theta(\eta) = \frac{T - T_{\infty}}{T_f - T_{\infty}}, \;\; \phi(\eta) = \frac{C - C_{\infty}}{C_w - C_{\infty}}, \;\; Ha_x = \frac{\sigma B_0^2}{\rho U_0}, \; Gr_x = \frac{g\beta(T_f - T_{\infty})x}{U_0^2},$$

$$Gc_x = \frac{g\beta^*(C_w - C_\infty)x}{U_0^2},\ Bi_x = \frac{h_f}{k}\sqrt{\frac{\upsilon x}{U_0}},\ \Pr = \frac{\upsilon}{\alpha},\ Sc = \frac{\upsilon}{D},\ S_x = \frac{Q_0 x}{U_0 \rho C_p},$$

$$Kr_x = \frac{Kr'x}{U_0},\ Nc = \frac{C_\infty}{C_w - C_\infty},\ R = \frac{4\sigma^* T_\infty^3}{3k^* k},\ \Omega = \frac{\upsilon}{Kc} \tag{9}$$

where prime denotes differentiation with respect to η, η is the similarity variable, $f(\eta)$ - the dimensionless stream function, $f'(\eta)$ - the dimensionless velocity, $\theta(\eta)$- the dimensionless temperature, $\varphi(\eta)$ - the dimensionless concentration Ha_x - the local magnetic field parameter, Gr_x - the local thermal Grashof number, Gc_x - the modified Grashof number, Ω - the permeability parameter, c- the stretching sheet parameter Bi_x - the local convective heat transfer parameter, Pr - the Prandtl number, Sc - the Schmidt number, S_x - the local heat source parameter, Kr_x - the local chemical reaction parameter, Nc - the concentration difference parameter and R - the radiation parameter.

In the view of the above similarity transformations, the equations (2), (8) and (4) reduce to

$$f''' + \frac{1}{2}ff'' - Ha_x f' + Gr_x\theta + Gc_x\phi - \Omega f'(\eta) \tag{10}$$

$$(1+4R)\theta'' + \frac{1}{2}\Pr\, f\theta' + \Pr S_x\theta = 0 \tag{11}$$

$$\varphi'' + \frac{1}{2}Scf\varphi' - ScKr_x(\varphi + Nc) = 0 \tag{12}$$

The corresponding boundary conditions are

$$f(0) = 0,$$

$$\theta'(0) = Bi_x\left[\theta(0) - 1\right],\ \varphi(0) = 1$$

$$f'(\infty) = 0,\ \theta(\infty) = 0,\ \varphi(\infty) = 0 \tag{13}$$

It can be noted that the local parameters Ha_x, Gr_x, Gc_x, Bi_x, and Kr_x and in (10) - (12) are functions of x and generate local similarity solution. In order to have a true similarity solution we assume the following relation [34]:

$$h_f = \frac{a}{\sqrt{x}},\ \sigma = \frac{b}{x},\ \beta = \frac{c}{x},$$

$$\beta^* = \frac{d}{x},\ Q_0 = \frac{e}{x},\ Kr' = \frac{m}{x} \tag{14}$$

where a, b, c, d, e and m are the constants with appropriate dimensions. In view of relation (2.14) the parameters, Ha_x, Gr_x, Gc_x, Bi_x, and Kr_x and are now independent of x and henceforth, we drop the index "x" for simplicity.

For the type of boundary layer flow under consideration, the skin-friction coefficient, Nusselt number and Sherwood number are important parameters. They are described as follows.

Knowing the velocity field, the shearing stress at the plate can be obtained, which in non-dimensional form (skin-friction coefficient) given by

$$C_f = \frac{2\tau_w}{\rho U_0^2} = \frac{2\mu}{\rho U_0^2}\left(\frac{\partial u}{\partial y}\right)_{y=0} = 2\,\mathrm{Re}_x^{-1/2}\, f''(0)$$

where Re_x is the Reynolds number and τ_w is the shear stress along the plate.

Knowing the temperature field, the heat transfer coefficient at the plate can be obtained, which in the non-dimensional form in terms of the Nusselt number, is given by

$$Nu = \frac{q_w x}{k\left(T_w - T_\infty\right)} = -\frac{x}{\left(T_w - T_\infty\right)}\left(\frac{\partial T}{\partial y}\right)_{y=0} = -\mathrm{Re}_x^{1/2}\,\theta'(0)$$

q_w is the surface heat.

Knowing the concentration field, the mass transfer coefficient at the plate can be obtained, which in the non-dimensional form in terms of the Sherwood number, is given by

$$Sh = \frac{q_m x}{k\left(C_w - C_\infty\right)} = -\frac{x}{\left(C_w - C_\infty\right)}\left(\frac{\partial C}{\partial y}\right)_{y=0} = -\mathrm{Re}_x^{1/2}\,\varphi'(0)$$

q_m is the surface mass.

3. SOLUTION OF THE PROBLEM

In this section, we present the numerical solution of the system of ordinary differential equations (10) - (12) subject to the boundary conditions (13). Equations (10) - (12) constitute a highly non linear coupled boundary value problem of third and second order and in general, difficult to solve analytically. So we develop most effective numerical shooting technique (Jain *et al*. [35]) with fourth-order-Runge-Kutta integration scheme with Newton Raphson Method. First of all, higher order non-linear differential equations (10) - (12) are converted into simultaneous linear differential equations of first order. The set of these equations are converted into an initial value problem by means of the shooting technique. The resultant equation is solved by Runge-Kutta fourth order method. As the criterion of convergence, in order to get six decimal place accuracy of numerical solution, the step size is taken as $\Delta\eta$=0.0001. From the process of numerical computation, the physical quantities such as the skin-friction coefficient, heat transfer coefficient, plate surface temperature and mass transfer coefficient are also obtained.

4. RESULTS AND DISCUSSIONS

In order to get a physical insight into the problem, a parametric study is conducted to illustrate the effects of different governing parameters viz ., the magnetic field parameter (*Ha*), the thermal Grashof number (*Gr*), the modified Grashof number (*Gc*), the permeability parameter (Ω), the convective heat transfer parameter (*Bi*), the Prandtl number(*Pr*),

the Schmidt number (*Sc*), the heat source parameter (*S*), the radiation parameter (*R*), the chemical reaction parameter(*Kr*) and concentration difference parameter (*Nc*) upon the nature of flow and transport, the numerical results are depicted graphically in Figs.2-21. Throughout the calculations, the parametric values are chosen as for *Ha*=0.1, *Gr*=*Gc*=0.1, Ω=0.5, *Bi*=0.1, *Pr*=0.72, *S*=0.02, *R*=0.1, *Kr*=0.1, *Sc*=0.62 and *Nc*=0.01. All the graphs therefore correspond to these values unless specifically indicated on the appropriate graph. Numerical results for the skin-friction coefficient, the Nusselt number, the Sherwood number and plate surface temperature for various values of physical parameters are reported in Tables.

In Figure 2 depicts the velocity distribution for different magnetic parameter (*Ha*) values. It is observed that as *Ha* increases, the velocity decreases. This is due to the fact that applied magnetic field gives rise to Lorentz force, which opposes the velocity. Figure 3 denotes the effect of *Ha* on the temperature. It is seen that the temperature of the fluid increases as *Ha* increases. This is due to the fact that applied magnetic field tends to heat the fluid, and thus reduces the heat transfer from the wall and simultaneously increases its concentration boundary layer is presented in Figure 4.

The effect of the convective heat transfer parameter (Bi_x) on the temperature is presented in Figure 5. It is seen that with an increase in the convective heat transfer parameter, the thermal boundary layer thickness increases with an increase in the plate surface convective heat parameter.

The effects of the thermal Grashof number (*Gr*) and mass (solutal) Grashof number (*Gc*) on the velocity field are shown in Figure 6 and Figure 7. It is found that the velocity increases with an increase in *Gr* and *Gc.* This is due to an increase in *Gr* and *Gc*, the thermal and mass buoyancy effects increases, hence surface cooling increases, results in increase in velocity. It can be seen that velocity increases near the plate and decreases smoothly away from the plate for increasing values of *Gc*. Figure 8 and Figure 9 illustrates the temperature distribution for different values of *Gr* and *Gc.* It can be seen that temperature decreases for increasing values of *Gr* and *Gc*. The effect of buoyancy parameters *Gr* and *Gc* on the concentration field is illustrated in Figure 10 and Figure 11. It is noticed that concentration boundary layer thickness decreases with an increase in the thermal or solutal Grashof numbers. It is due to fact that an increase in *Gc* and *Gr*, increases the mass buoyancy effect, and there by induced flow increase and hence concentration increases.

Figures 12-14 display the effect of the permeability parameter (Ω) on the velocity, temperature and concentration distributions. As shown in the figures, the temperature and concentration are increasing with increasing the dimensionless permeability parameter and the velocity decreases as Ω increases. It is observed that, the velocity decreases as the permeability parameter increases. The parameter Ω is inversely proportional to the actual permeability *K* of the porous medium. Hence an increase in Ω will increase the resistance of the porous medium (as the permeability physically becomes more) which will tend to decelerate the flow and thereby reduce its velocity.

Figure 15 shows the effect of the Prandtl number (*Pr*) on the temperature. The Prandtl number defines the ratio of momentum diffusivity to thermal diffusivity. It is can be seen that with an increase in *Pr*, the temperature decreases. This is because, physically, if Prandtl number increases, the thermal diffusivity decreases equivalent to increase the thermal conductivities, and therefore heat is able to diffuse away from the heated surface more rapidly than for higher values of *Pr* that reduces the thermal boundary layer.

Figure 16 depicts the temperature distribution for various values of thermal radiation parameter (*R*). It can be seen that as *R* increases there is an increase in thermal boundary layer.

Figure 17 shows the variation of the temperature with the heat source parameter (*S*). It is noticed that as heat

source parameter increases, temperature increases. The presence of heat source rise in the heat generation causes an increase in the thermal state of the fluid and hence thermal boundary layer increases.

Figure 18 shows the variation of the concentration profile for different values of chemical reaction parameter (*Kr)*.It is seen that as *Kr* increases, concentration decreases. This is because when *Kr* increases the bonds between atoms will break up and thereby dilutes the concentration of the fluid.

The effect of chemical reaction parameter (*Kr*) on the concentration is presented in Figure 18. It is observed that the species concentration decreases with an increase in the chemical reaction parameter. Physically this shows that an increase in chemical reaction parameter breaks up the bonds between the atoms and thus the density of the species dilutes and thereby decreases the concentration of the fluid.

The variation in the velocity and concentration boundary layer of the flow field for different values of Schmidt number are shown in Figure 19 and Figure 20. The effect of Schmidt number is to decrease the concentration distribution of the flow field. It is further found that the decrease in the concentration boundary layer of the flow field is more significant in presence of heavier diffusing species. This causes buoyancy effects to decrease yielding reduction in the velocity.

The effect of the concentration difference parameter (*Nc*) on the temperature is shown in Figure 21. It can be seen that, an increase in the concentration difference parameter decreases the concentration.

Numerical results for the skin-friction coefficient, the Nusselt number, Sherwood number and plate surface temperature for various values of physical parameters are reported in Tables. It is observed that in absence of radiation parameter and the permeability parameter that is, for $R=0$ and $\Omega=0$; (10), (11) and (12) together with boundary condition (13) are the same as those obtained by Rout [36]. The present results are compared with that of Rout et al [37] for the skin friction coefficient, Nusselt numbers, plate surface temperature and Sherwood number in Table 1 for reduced case $R=\Omega=0$ and found that there is an excellent agreement.

From Table 2, an increase in the local convective heat transfer parameter shows an increasing trend in the local skin friction coefficient, heat transfer coefficient, mass transfer coefficient and plate surface temperature. It is observed as magnetic parameter increases, the plate surface temperature increase while the skin friction, rates of heat and mass transfer decrease. It can be seen that with an increase in the permeability parameter, the skin friction coefficient, rates of heat and mass transfer coefficients decrease, where as the plate surface temperature increases.

From of Table 3, it is noticed that as the radiation parameter increases, the skin friction coefficient, plate surface temperature and Sherwood number increase where as the Nusselt number decreases. With the data in the next four rows of Table 3, it is seen that as the Prandtl number increases, there is a rise in the Nusselt number and fall in the skin friction coefficient, the plate surface temperature and Sherwood number. With the data in the last four rows of the Table 3 it is observed that as heat source parameter increases the skin friction coefficient, plate surface temperature and Sherwood number increase while the Nusselt number decreases.

From Table 4 it is clear that both the skin friction coefficient and Nusselt number decrease while the plate surface temperature increase and Sherwood number increases very rapidly as the Schmidt number or chemical reaction parameter or concentration difference parameter increases.

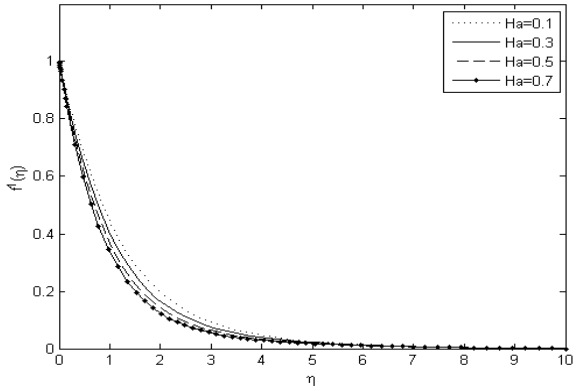

Figure 2: Velocity Profiles for Different Values of *Ha*

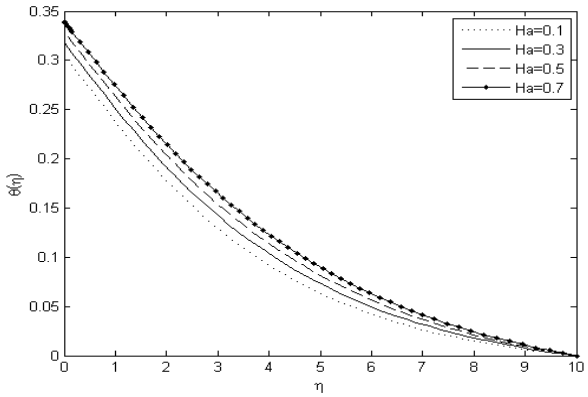

Figure 3: Temperature Profiles for Different Values of *Ha*

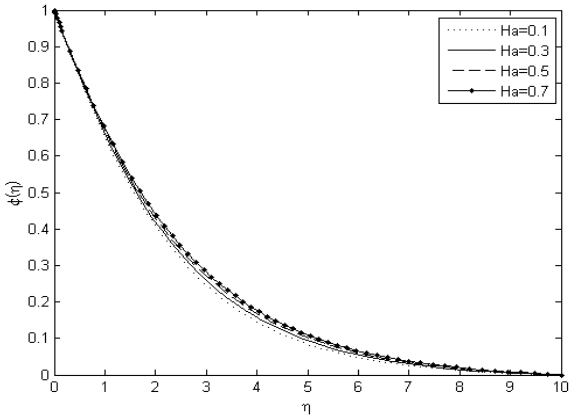

Figure 4: Concentration Profiles for Different Values of *Ha*

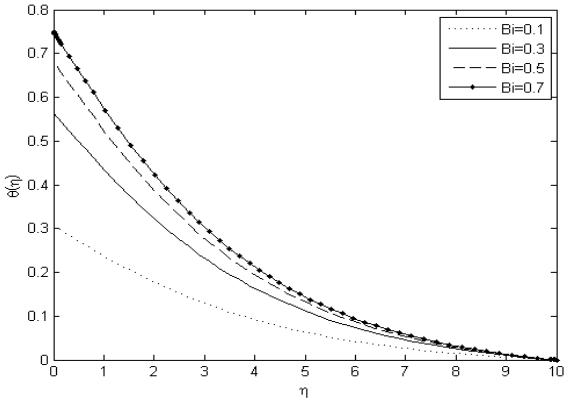

Figure 5: Temperature Profiles for Different Values of *Bi*

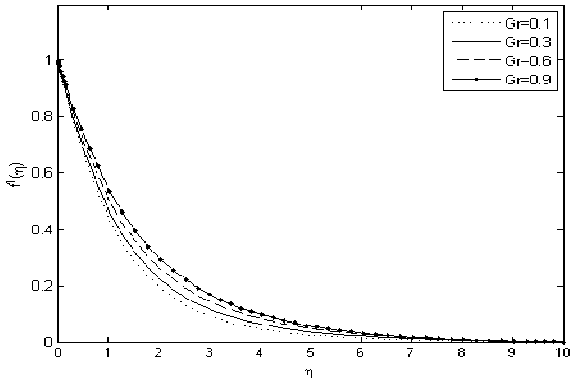

Figure 6: Velocity Profiles for Different Values of *Gr*

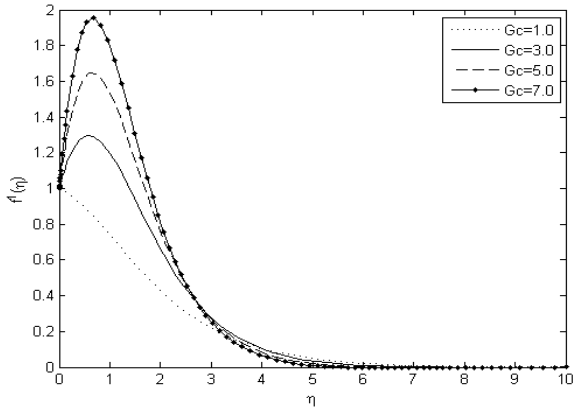

Figure 7: Velocity Profiles for Different Values of *Gc*

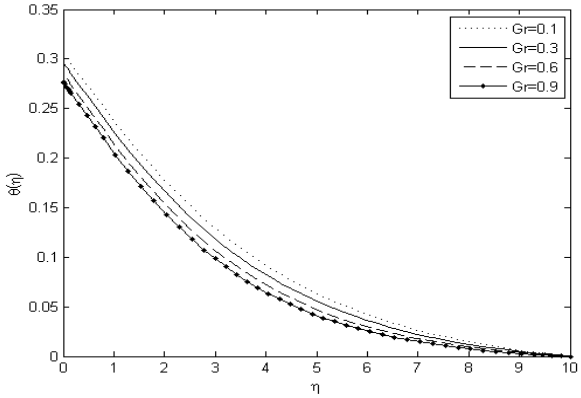

Figure 8: Temperature Profiles for Different Values of *Gr*

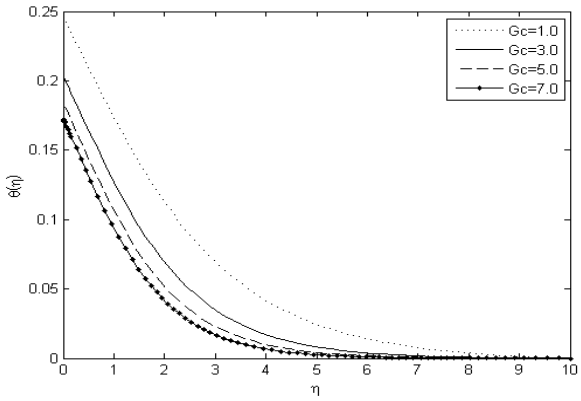

Figure 9: Temperature Profiles for Different Values of *Gc*

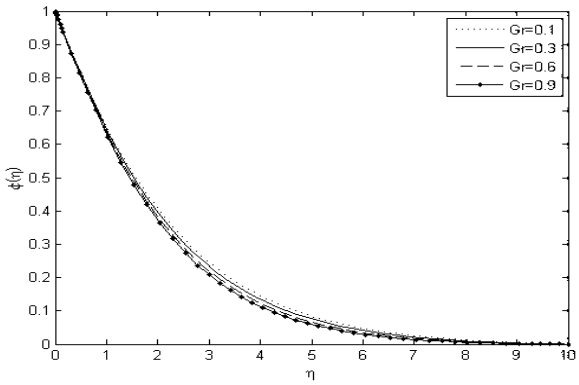

Figure 10: Concentration Profiles for Different Values of *Gr*

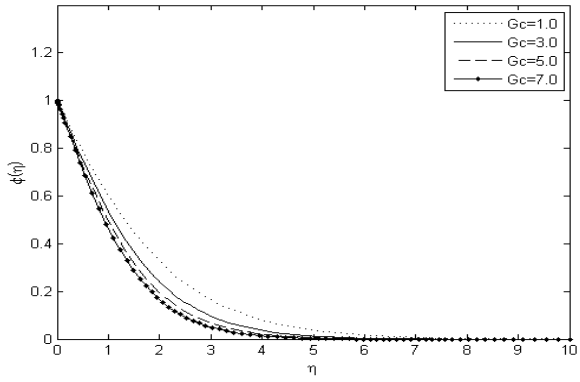

Figure 11: Concentration Profiles for Different Values of *Gc*

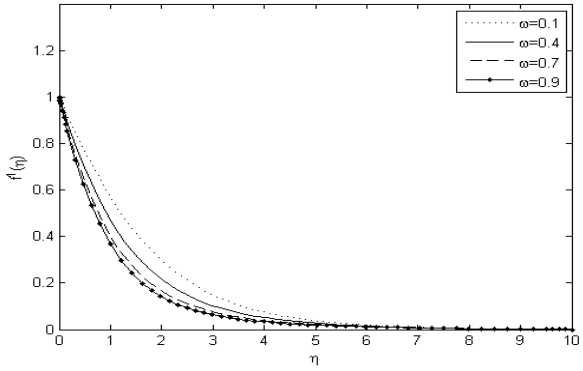

Figure 12: Velocity Profiles for Different Values of *ω*

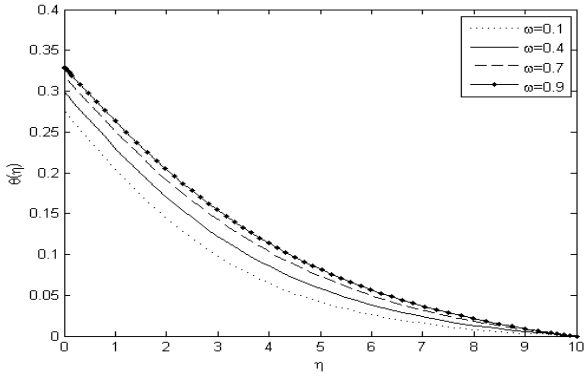

Figure 13: Temperature Profiles for Different Values of *ω*

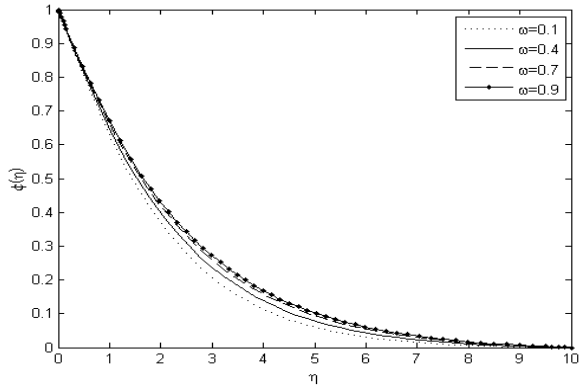

Figure 14: Concentration Profiles for Different Values of ω

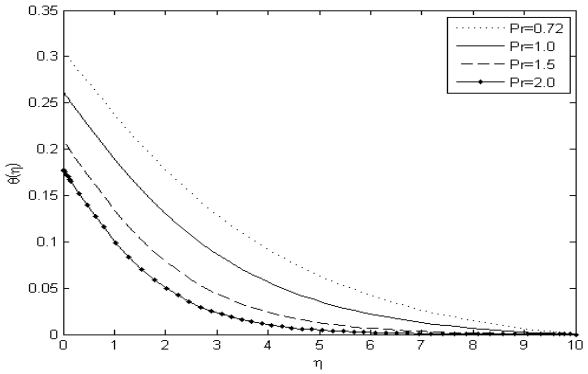

Figure 15: Temperature Profiles for Different Values of *Pr*

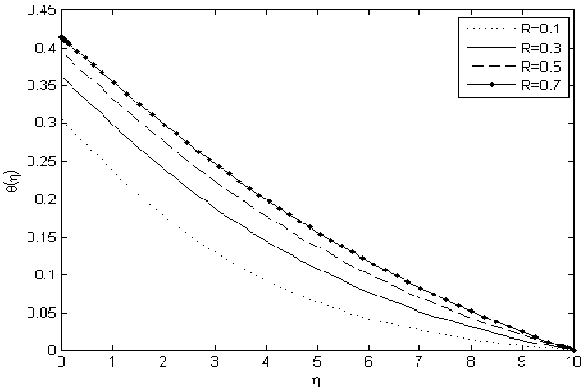

Figure 16: Temperature Profiles for Different Values of *R*

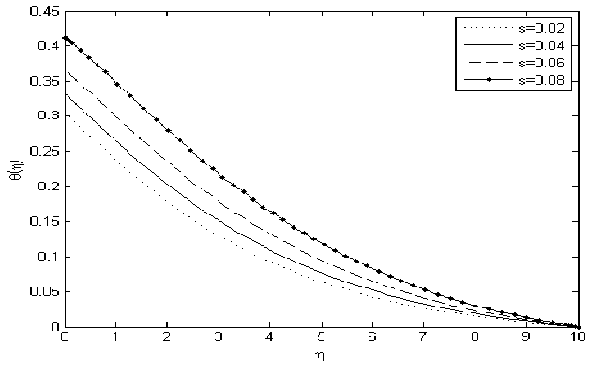

Figure 17: Temperature Profiles for Different Values of *s*

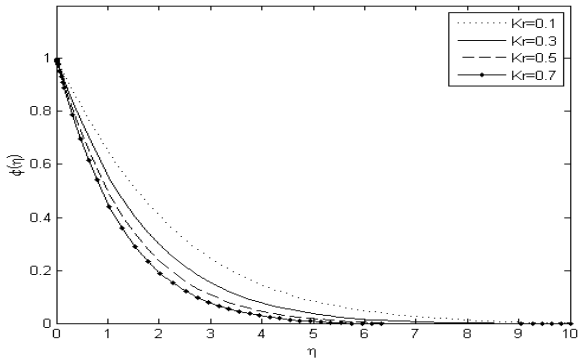

Figure 18: Concentration Profiles for Different Values of *Kr*

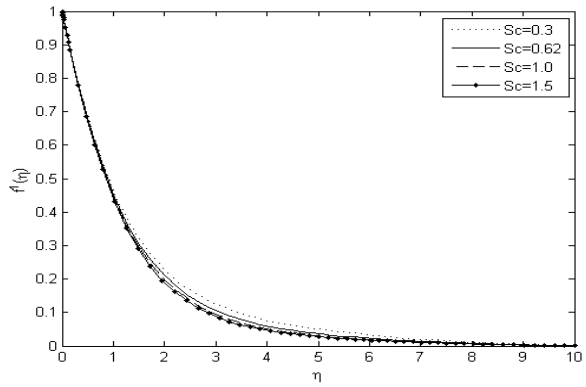

Figure 19: Velocity Profiles for Different Values of *Sc*

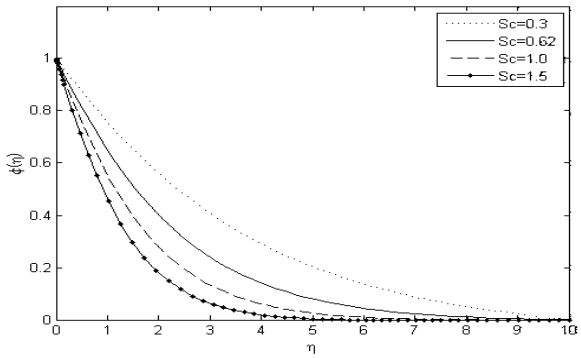

Figure 20: Concentration Profiles for Different Values of *Sc*

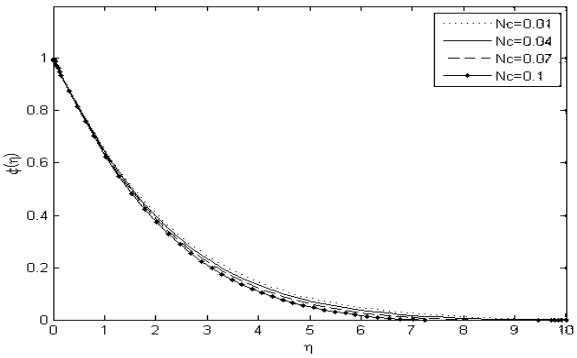

Figure 21: Concentration Profiles for Different Values of *Nc*

Table1: Comparison of the Present Results with that of Rout *et al.* [36]

Bi	*Gr*	*Gc*	*Ha*	*Pr*	*Sc*	$f''(0)$	$-\theta'(0)$	$\theta(0)$	$-\varphi'(0)$	$f''(0)$	$-\theta'(0)$	$\theta(0)$	$-\varphi'(0)$
0.1	0.1	0.1	0.1	0.72	0.62	-0.402271	0.078635	0.213643	0.3337425	-0.402271	0.078635	0.213643	0.333742
1.0	0.1	0.1	0.1	0.72	0.62	-0.352136	0.273153	0.726846	0.3410294	-0.352136	0.273153	0.726846	0.341029
0.1	0.5	0.1	0.1	0.72	0.62	-0.322212	0.079173	0.208264	0.3451301	-0.322212	0.079173	0.208264	0.345130
0.1	1.0	0.1	0.1	0.72	0.62	-0.231251	0.079691	0.203088	0.3566654	-0.231251	0.079691	0.203088	0.356665
0.1	0.1	0.5	0.1	0.72	0.62	-0.026410	0.080711	0.192889	0.3813954	-0.026410	0.080711	0.192889	0.381395
0.1	0.1	1.0	0.1	0.72	0.62	-0.379918	0.082040	0.179592	0.4176699	-0.379918	0.082040	0.179592	0.417669
0.1	0.1	0.1	0.1	1.0	0.62	-0.407908	0.081935	0.180640	0.3325180	-0.407908	0.081935	0.180640	0.332518
0.1	0.1	0.1	0.1	0.72	0.78	-0.411704	0.078484	0.215159	0.3844559	-0.411704	0.078484	0.215159	0.384455

Table 2: Numerical Values of the Skin Friction $f''(0)$, Nusselt Number $-\theta'(0)$, plate Surface Temperature $\theta(0)$, and the Sherwood Number $-\varphi'(0)$ for *Kr*=0.1, *Nc*=0.01, *Pr*=0.72, *R=0.1*

***S*=0.02 and *Sc*=0.62**

Bi	*Ha*	*Gc*	*Gr*	*Ω*	$f''(0)$	$-\theta'(0)$	$\theta(0)$	$-\varphi'(0)$
0.1	0.1	0.1	0.1	0.5	-0.767385	0.069413	0.305626	0.388505
0.15	0.1	0.1	0.1	0.5	-0.738092	0.130827	0.561797	0.391220
0.2	0.1	0.1	0.1	0.5	-0.325170	0.169380	0.828240	0.393031
0.1	0.1	0.1	0.1	0.5	-0.764439	0.069432	0.305190	0.388505
0.1	0.3	0.1	0.1	0.5	-0.870754	0.068214	0.317161	0.379190
0.1	0.5	0.1	0.1	0.5	-0.968835	0.067114	0.328202	0.371777
0.1	0.1	1.0	0.1	0.5	-0.129323	0.075371	0.245259	0.445081
0.1	0.1	3.0	0.1	0.5	1.070647	0.079649	0.202370	0.516541
0.1	0.1	5.0	0.1	0.5	2.133467	0.081573	0.183059	0.563180
0.1	0.1	0.1	0.1	0.5	-0.761495	0.069450	0.304754	0.388103
0.1	0.1	0.1	0.3	0.5	-0.709114	0.070423	0.294986	0.394949
0.1	0.1	0.1	0.6	0.5	-0.637631	0.071529	0.283882	0.403611
0.1	0.1	0.1	0.1	0.1	-0.489237	0.072482	0.274315	0.413471
0.1	0.1	0.1	0.1	0.4	-0.701358	0.070133	0.297895	0.393351
0.1	0.1	0.1	0.1	0.7	-0.870754	0.068214	0.317161	0.379190

Table 3: Numerical Values of the Skin Friction $f''(0)$, Nusselt number $-\theta'(0)$, Plate Surface Temperature θ (0), and the Sherwood Number $-\varphi'(0)$ for Bi=0.1, Gr=0.1, Gc=0.1, Ha=0.1, Kr=0.1

Nc=0.01 and Ω=0.5

R	Pr	S	$f''(0)$	$-\theta'(0)$	$\theta(0)$	$-\varphi'(0)$
0.1	0.72	0.02	-0.761495	0.069450	0.304754	0.388103
0.3	0.72	0.02	-0.753944	0.063840	0.360824	0.389539
0.5	0.72	0.02	-0.749542	0.060644	0.392760	0.390400
0.7	0.72	0.02	-0.746566	0.058509	0.414096	0.390991
0.1	0.72	0.02	-0.761495	0.069450	0.304754	0.388103
0.1	1.0	0.02	-0.767263	0.073882	0.260445	0.387056
0.1	1.5	0.02	-0.773714	0.079086	0.208419	0.385965
0.1	2.0	0.02	-0.777429	0.082288	0.176425	0.385397
0.1	0.72	0.02	-0.761495	0.067450	0.304754	0.388103
0.1	0.72	0.04	-0.758330	0.066935	0.330645	0.388642
0.1	0.72	0.06	-0.754147	0.063626	0.364635	0.389356
0.1	0.72	0.08	-0.748383	0.059085	0.411204	0.390343

Table 4: Numerical Values of the Skin Friction $f''(0)$, Nusselt Number $-\theta'(0)$, plate Surface Temperature $\theta(0)$, and the Sherwood Number $-\varphi'(0)$ for Bi=0.1, Gc=0.1, Gr=0.1, Ha=0.1, Kr=0.1

Pr=0.72, R=0.1 and Ω=0.5

Kr	Sc	Nc	$f''(0)$	$-\theta'(0)$	$\theta(0)$	$-\varphi'(0)$
0.1	0.62	0.01	-0.761495	0.069450	0.304754	0.388103
0.3	0.62	0.01	-0.770394	0.069116	0.308111	0.532169
0.5	0.62	0.01	-0.775927	0.068930	0.309977	0.641540
0.7	0.62	0.01	-0.779929	0.068807	0.311205	0.733205
0.1	0.3	0.01	-0.734050	0.059021	0.408964	0.260130
0.1	0.62	0.01	-0.746718	0.058618	0.413006	0.390961
0.1	1.0	0.01	-0.756418	0.058365	0.415538	0.516581
0.1	1.5	0.01	-0.764834	0.058190	0.417298	0.653738
0.1	0.62	0.01	-0.761495	0.069450	0.304754	0.388103
0.1	0.62	0.04	-0.762296	0.069405	0.305210	0.395348
0.1	0.62	0.07	-0.763097	0.069359	0.305671	0.402600
0.1	0.62	0.1	-0.763900	0.069312	0.306136	0.409860

CONCLUSIONS

This paper analyzes the effect of thermal radiation on MHD free convective flow over a moving vertical plate embedded in a porous medium in the presence of heat source and chemical reaction with convective surface boundary condition. The results and discussion of the present study leads to the following observations.

- An increase in the magnetic parameter enhances the temperature, concentration, Skin friction coefficient, Nusselt number, plate surface temperature, and Sherwood number but reduces the velocity.
- Increase in the convective heat transfer parameter increases the temperature, the skin-friction coefficient, Nusselt number, Sherwood number and plate surface temperature.
- An increase in the permeability parameter leads to an increase in the temperature, concentration and plate surface temperature and decrease in the velocity, skin-friction coefficient, Nusselt number and Sherwood number.
- As mass (solutal) Grashof increases the velocity increases near the plate and then it decreases smoothly away

from the plate, while the velocity increases throughout the boundary layer with an increase in the thermal Grashof number.

- An increase in the mass (solutal) Grashof or thermal Grashof number causes a fall in the temperature, the concentration as well as the plate surface temperature, whereas rise in the skin friction coefficient, Nusselt number and Sherwood number.
- As the Prandtl number increases, the temperature, skin friction coefficient, plate surface temperature and Sherwood number decrease while the Nusselt number increases.
- There is an increase in the thermal boundary layer thickness, the skin friction coefficient, plate surface temperature and Sherwood number while the Nusselt number decreases with an increase in the radiation parameter or heat source parameter.
- As the chemical reaction parameter or the concentration difference parameter or Schmidt number increases there is an increase in the plate surface temperature and Sherwood number while decrease in the concentration, skin friction coefficient and Nusselt number.
- An increase in the Schmidt number leads to a decre ase in the velocity.

REFERENCES

1. Bejan, A. and Khair, K.R., (1985), Heat and mass transfer by natural convection in a porous medium, International Journal of Heat Mass Transfer, Vol. 28, pp.909-918.
2. Lai, F.C. and Kulacki, F.A., (1990), Coupled heat and mass transfer from a sphere buried in an infinite porous medium, International Journal of Heat Mass Transfer, Vol. 33, pp.209-215.
3. Raptis A., Tzivanidis G. and Kafousias N., (1981), Free convection and mass transfer flow through a porous medium bounded by an infinite vertical limiting surface with constant suction, Lett. Heat Mass Transfer, Vol.8, pp.417-424.
4. Lai, F.C. and Kulacki, F.A.. (1991), Coupled heat and mass transfer by natural convection from vertical surfaces in a porous medium, International Journal of Heat Mass Transfer, Vol.34, pp.1189-1194.
5. Huges W. F and Young F. J (1966), The Electro-Magneto Dynamics of fluids, John Wiley and Sons, New York.
6. Shanker, B. and Kishan, N., (1997), The effects of mass transfer on the MHD flow past an impulsively started infinite vertical plate with variable temperature or constant heat flux, J. Eng. Heat Mass Transfer, Vol.19, pp.273-278.
7. Bhaskara Reddy, N. and Bathaiah, D., (1981), Magnetohydrodynamic free convection laminar flow of an incompressible viscoelastic fluid, Reg. J. of Energy Heat Mass Transfer, Vol.3, No.4, pp.239-255.
8. Bhaskara Reddy, N. and Bathaiah, D., (1982), MHD combined free and forced convection flow through two parallel porous walls, Acta Mechanica, Vol.42, pp.239-251.
9. Elabashbeshy, E.M.A. (1997), Heat and mass transfer along a vertical plate with variable temperature and concentration in the presence of magnetic field, Int. J. Eng. Sci., Vol.34, pp.515-522.

10. Helmy, K.A., (1998), MHD Unsteady free convection flow past a vertical porous plate. Journal of Applied Mathematics and Mechanics 78, 255-270.

11. Hossain, M.A. and Takhar, H.S., (1996), Radiation effect on mixed convection along a vertical plate with uniform surface temperature, Heat and Mass Transfer, vol. 31, pp. 243–248.

12. Suneetha, S., Bhaskar Reddy, N. and Ramchandra Prasad, V., (2008), The thermal radiation effects on MHD free convection flow past an impulsively started vertical plate with variable surface temperature and concentration", Journal of Naval Architecture and Marine engineering, vol. 2, pp. 57 – 70.

13. Chandrakala, P., (2010), Radiation effects on flow past an impulsively started vertical oscillating plate with uniform heat flux", International Journal of Dynamics of Fluids, vol. 6, pp. 209–215.

14. Anki Reddy, P. and Bhaskar Reddy, N., (2011), Thermal radiation effects on hydro-magnetic flow due to an exponentially stretching sheet, International Journal of Applied Mathematics and Computer, vol. 3, pp. 300-306.

15. Raptis, A. (1998), Radiation and free convection flow through a porous medium, Int. comm. Heat and Mass Transfer, Vol. 25(2), pp.289-295.

16. Anuar Ishak, (2011), MHD boundary layer flow due to an exponentially stretching sheet with radiation effect, Sains Malaysiana, Vol. 40, no. 4, pp. 391–395.

17. Mansour, M. H., (1990), Radiative and free convection effects on the oscillatory flow past a vertical plate, Astrophysics and space science, Vol.166, pp.26-75.

18. Sajid, M. and Hayat, T., (2008), Influence of thermal radiation on the boundary layer flow due to an exponentially stretching sheet, International Communications in Heat Mass Transfer, Vol.35, pp.347-356.

19. Bidin, B. & Nazar, R., (2009), Numerical solution of the boundary layer flow over an exponentially stretching sheet with thermal radiation, European Journal of Scientific Research, Vol.33, no.4, pp.710-717.

20. Poornima, T. and Bhaskar Reddy, N., (2013), Radiation effects on MHD free convective boundary layer flow of nanofluids over a nonlinear stretching sheet, Advances in Applied Science Research, Pelagia Research Library, Vol. 4, no. 2, pp. 190-202

21. Makinde O.D., (2005), Free-convection flow with thermal radiation and mass transfer past a moving vertical porous plate, Int. Comm. Heat Mass Transfer 32: 1411-1419.

22. Das, U. N., Deka, R. and Soundalgekar, V. M., (1994), Effects of mass transfer on flowpast an impulsively started infinite vertical plate with constant heat flux and chemical reaction, Forschung im Ingenieurwesen/Engineering Research, vol. 60, no. 10, pp. 284–287.

23. Anjalidevi S. P. and Kandasamy, R., (1999), Effects of chemical reaction, heat and mass transfer on laminar flow along a semi infinite horizontal plate, Heat andMass Transfer, vol. 35, no. 6, pp. 465–467.

24. Seddeek, M. A., Darwish, A. A. and Abdelmeguid, M. S., (2007), Effects of chemical reaction and variable viscosity on hydromagnetic mixed convection heat and mass transfer for Hiemenz flow through porous media with radiation, Communications in Nonlinear Science and Numerical Simulation, vol. 12, no. 2, pp. 195–213.

25. Patil P. M. and Kulkarni, P. S., (2008), Effects of chemical reaction on free convective flow of a polar fluid through a porous mediumin the presence of internal heat generation," International Journal of Thermal Sciences, vol. 47, no. 8, pp. 1043–1054.

26. Gangadhar, K. and Bhaskar Reddy, N., (2013), Chemically Reacting MHD Boundary Layer Flow of Heat and Mass Transfer over a Moving Vertical Plate in a Porous Medium with Suction, Journal of Applied Fluid Mechanics, Vol. 6, no. 1, pp. 107-114.

27. Ramana Reddy, G. V.,. Ramana Murthy Ch. V. and Bhaskar Reddy, N., (2010), Mass transfer and radiation effects of unsteady MHD free convective fluid flow embedded in porous medium with heat generation/absorption, Journal of Applied Mathematics and Fluid Mechanics, Vol. 2, No. 1, pp. 85 – 98.

28. Olanrewaju, P. O., Arulogun, O. T. and Adebimpe, K., (2012), Internal heat generation effect on thermal boundary layer with a convective surface boundary condition, American Journal of Fluid Dynamics, vol. 2, no. 1, pp. 1–4.

29. Makinde, O.D., (2010), On MHD heat and mass transfer over a moving vertical plate with a convective surface boundary condition, Canadian Journal of Chemical Engineering, vol. 88, no. 6, pp. 983–990.

30. Makinde, O. D., (2011), Similarity solution for natural convection from a moving vertical plate with internal heat generation and a convective boundary condition, Thermal Science, vol. 15, supplement 1, pp. S137–S143.

31. Ibrahim, F. S., Elaiw, A. M. and Bakr, A.A. (2008), Effect of the chemical reaction and radiation absorption on the unsteady MHD free convection flow past a semi infinite vertical permeable moving plate with heat source and suction, Communications in Nonlinear Science and Numerical Simulation, vol. 13, no. 6, pp.1056–1066.

32. Salem, A. M. and Abd El-Aziz, M. (2008), Effect of Hall currents and chemical reaction on hydromagnetic flow of a stretching vertical surface with internal heat generation/absorption, Applied Mathematical Modelling, vol. 32, no. 7, pp. 1236–1254.

33. Brewster, M.Q., (1992), Thermal radiative transfer and properties, John Wiley & Sons, NewYork.

34. Makinde, O.D. (2010), On MHD heat and mass transfer over a moving vertical plate with a convective surface boundary condition, Canadian Journal of Chemical Engineering, vol. 88, no. 6, pp. 983–990.

35. Jain, M.K., Iyengar, S.R.K. and Jain, R.K., (1985), Numerical Methods for Scientific and Engineering Computation, Wiley Eastern Ltd., New Delhi, India

36. Rout, B. R., Parida, S. K. and Panda, S.,(2013), MHD Heat and Mass Transfer of Chemical Reaction Fluid Flow over a Moving Vertical Plate in Presence of Heat Source with Convective Surface Boundary Condition, International Journal of Chemical Engineeringhttp://dx.doi.org/10.1155/2013/296834.